

## Ce<sup>3+</sup> luminescent centers of different symmetries in KMgF<sub>3</sub> single crystals

R. Francini, U. M. Grassano, and L. Landi

*Dipartimento di Fisica and Istituto Nazionale di Fisica della Materia, Università di Roma "Tor Vergata,"  
Via della Ricerca Scientifica 1, 00133 Roma, Italy*

A. Scacco and M. D'Elena

*Dipartimento di Fisica and Istituto Nazionale di Fisica della Materia, Università di Roma "La Sapienza,"  
Piazzale Aldo Moro 2, 00185 Roma, Italy*

M. Nikl and N. Cechova

*Institute of Physics, Czech Academy of Sciences, Cukrovarnicka 10, 16200 Prague, Czech Republic*

N. Zema

*Istituto di Struttura della Materia del Consiglio Nazionale delle Ricerche, Via Enrico Fermi, 00044 Frascati, Italy*

(Received 18 June 1997)

Absorption, emission, and excitation spectra of KMgF<sub>3</sub> doped with Ce<sup>3+</sup> have been measured in the near ultraviolet up to 180 nm. In this fluoroperovskite lattice, absorption of the Ce<sup>3+</sup> impurity is found at energies higher than 4.4 eV. Broad-band emissions are measured at 350 nm and 275 nm which are identified as the 5*d*→4*f* radiative recombination at two different Ce<sup>3+</sup> centers. The same substitutional site is proposed for both centers, with the unperturbed site rapidly saturating with an increasing concentration of Ce<sup>3+</sup> in favor of a site perturbed by two K<sup>+</sup>-ion vacancies. [S0163-1829(97)01447-1]

### I. INTRODUCTION

The investigation of Ce<sup>3+</sup> ion impurity hosted in different fluoride crystals started almost thirty years ago<sup>1</sup> and is continuing up to now.<sup>2</sup> The main reasons of such unending interest among solid-state physicists, material scientists, and laser engineers are twofold. On one side Ce<sup>3+</sup> is a model case: the simplest rare-earth (RE) ion (with only one optically active 4*f* electron) hosted in wide band-gap crystals allows a complete investigation of all its spectroscopic properties. On the other side, the broad-band UV emission has been used to develop tunable solid-state lasers,<sup>3-6</sup> amplifiers,<sup>2</sup> and efficient scintillators,<sup>7,8</sup> while the search for new and more efficient materials for an optoelectronic device is still going on.

The model case for the study of optical properties of RE encountered very soon unexpected complications: the host fluorides of early works were mostly alkaline-earth fluorides where the Ce<sup>3+</sup> ion substitutes a divalent alkaline-earth ion introducing charge compensating F<sup>-</sup> interstitials and producing centers with different lattice symmetries around the Ce<sup>3+</sup> ion.<sup>9</sup> The complications due to charge compensation can be avoided in those crystals which contain a trivalent host ion. The system LaF<sub>3</sub>-CeF<sub>3</sub> has been thoroughly investigated for example by Elias, Heaps, and Yen<sup>10</sup> and by Pedrini, Moine, Gacon, and Jacquier.<sup>8</sup> The local symmetry of the Ce<sup>3+</sup> in these tysonite structures is very low (*C*<sub>2</sub>) and also in these systems perturbed sites are very likely to occur.

On the applicative side, the exploitation in a laser of the very high quantum efficiency of practically all the RE ions must fulfill a resonant condition between the Ce<sup>3+</sup> absorption bands and the pumping lines of the available excimer lasers. Moreover the mechanical and thermal properties of

the host crystal must withstand the pumping intensity (no self-focusing) and the energy of the UV photons (no color center formation). LaF<sub>3</sub>,<sup>3</sup> LiYF<sub>4</sub>,<sup>3,4</sup> LuLiF<sub>4</sub>,<sup>2</sup> LiCaAlF<sub>6</sub>,<sup>11,12</sup> and LiSrAlF<sub>6</sub>,<sup>13</sup> all doped with Ce<sup>3+</sup> have proved successful in yielding large gain and tunable output. In this framework we investigated Ce<sup>3+</sup> ions in a different system: the fluoroperovskite KMgF<sub>3</sub>. Only ESR measurements<sup>14</sup> are reported in this host crystal indicating the presence of different sites for the impurity, but no optical experiments were performed. In this work we report the investigation of optical absorption, emission (spectra and lifetime), one-photon excitation up to about 7 eV and two-photon excitation. The latter technique has been widely used in this field of research.<sup>8,15-17</sup> Even if, as explained below, the main Ce<sup>3+</sup>-ion transitions are one-photon allowed and two-photon forbidden, the mixing of electronic wave functions by the host crystal-field makes two-photon transitions observable yielding a higher spectroscopic accuracy and different symmetry data through the polarization dependence of the two-photon excitation.

A schematic diagram of the levels of the Ce<sup>3+</sup> ion in different symmetries is drawn in Fig. 1. The free-ion calculated levels are reviewed by Dieke<sup>18</sup> and are shown on the left-hand side of the figure. The spin-orbit interaction splits the 4*f* ground state into two levels <sup>2</sup>F<sub>7/2</sub> and <sup>2</sup>F<sub>5/2</sub>, separated by approximately 2000 cm<sup>-1</sup>; the 5*d* level, approximately 51 000 cm<sup>-1</sup> above the ground state, is split into <sup>2</sup>D<sub>5/2</sub> and <sup>2</sup>D<sub>3/2</sub> distant about 1000 cm<sup>-1</sup>; the 6*s* level is around 86 000 cm<sup>-1</sup>. For the Ce<sup>3+</sup> ion, a cubo-octahedral site, as we shall see below, is the most probable substitutional site. The 5*d* level is split by the weak crystal field into the two *e*<sub>g</sub> and *t*<sub>2g</sub> bands in the order as indicated. If we further apply a weak spin-orbit interaction the *t*<sub>2g</sub> level should further split into the Γ<sub>7</sub> and Γ<sub>8</sub> components. In the

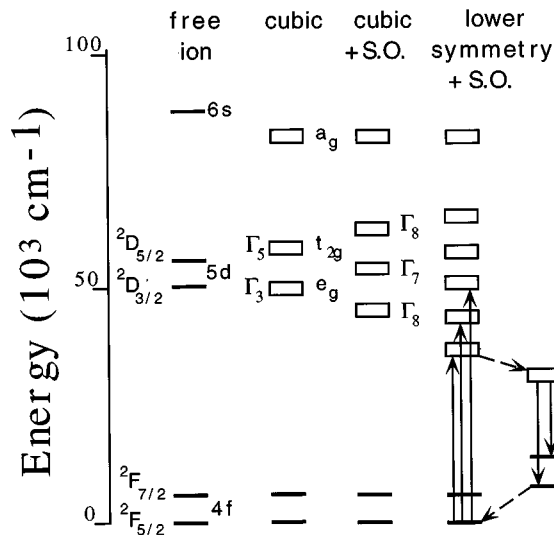


FIG. 1. Schematic energy levels of  $\text{Ce}^{3+}$  ion. Levels on the right represent the ion in a symmetry lower than cubic (perturbed site) with the relevant optical transitions indicated by solid arrows (radiative) and dashed arrows (nonradiative).

case of a large crystal field of lower symmetry, such as, for example, that produced by the presence of charge compensating interstitials or cation vacancies, the degeneracy of the  $5d$  level is completely removed as shown by the 5 Kramers doublets on the right-hand side of Fig. 1. The total splitting of the  $5d$  manifold varies in the different fluoride hosts from  $7000 \text{ cm}^{-1}$  to  $14000 \text{ cm}^{-1}$  and therefore the effects of the crystal field are much larger than those of the spin-orbit interaction. The  $\text{KMgF}_3$  lattice has two positive ion sites: the  $\text{Mg}^{2+}$  site in an octahedral configuration with 6  $\text{F}^-$  nearest neighbors and the  $\text{K}^+$  site with cubo-octahedral symmetry and 12  $\text{F}^-$  nearest neighbors. As will be discussed below the most likely site for the  $\text{Ce}^{3+}$  ion is the  $\text{K}^+$  substitutional site.

## II. EXPERIMENT

$\text{KMgF}_3:\text{Ce}^{3+}$  single crystals were grown from the melt with the Kyropoulos method in inert atmosphere starting from stoichiometric mixtures of  $\text{KF}$  and  $\text{MgF}_2$  dehydrated powders added of various amounts of  $\text{CeF}_3$ . The single-crystal samples were cut and polished from the crystal boules (typical diameter of 2.5 cm and length of 3 cm) in the shape of slabs 1 mm to 2 mm thick and then mounted on the cold finger of a variable temperature (15–300 K) cryostat. Absorption spectra were performed with a double-beam spectrometer Lambda-19 (Perkin-Elmer). Luminescence and excitation spectra were acquired with a PAR optical multichannel analyzer equipped with a 30-cm focal length monochromator. The excitation sources were a xenon or a deuterium CW lamp. Part of the spectroscopic investigation on  $\text{KMgF}_3:\text{Ce}^{3+}$  was performed at the VUV synchrotron-light facility of Hasylab at Desy (Hamburg, Germany). Two-photon transitions were detected by monitoring the  $\text{Ce}^{3+}$  luminescence which follows the excitation process. The exciting source was a dye laser pumped by an excimer laser (Lambda-Physik EMG-103 plus FL-2001), which delivers pulses of 8–10 ns duration and peak powers from 200 kW to

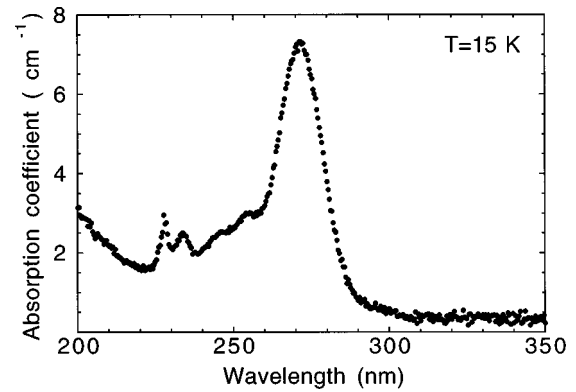


FIG. 2. Absorption spectrum of  $\text{KMgF}_3:\text{Ce}^{3+}$  at low temperature. Nominal doping in the melt was 0.05 mol% of  $\text{CeF}_3$ .

350 kW, at a repetition rate of 20 Hz.  $\text{Ce}^{3+}$  fluorescence decays were measured by Spectrofluorometer 199S (Edinburgh Instrument), which uses a hydrogen filled coaxial flashlamp as an excitation source and single-photon counting detection. A deconvolution procedure was applied to the measured decays to extract the true decay times.

## III. RESULTS

### A. Absorption

A typical absorption spectrum of  $\text{Ce}^{3+}$  doped  $\text{KMgF}_3$  at low temperature (15 K) is shown in Fig. 2. At least five absorption bands can be identified with peaks at 271, 255, 245, 234, and 227 nm. All the peaks show a small redshift ( $\sim 2 \text{ nm}$ ) when the temperature is increased to 300 K. The half width of the absorption bands can be determined with uncertainty due to the overlapping of the bands and to the presence of a sizable scattering background. The measured half width of the lowest-energy band is 0.30 eV at 15 K and 0.37 eV at room temperature. The sample used in the measurements of Fig. 2 was cleaved from a crystal with nominal doping (in the melt) of 0.05 mol% of  $\text{CeF}_3$ . The dependence of the heights of the bands on the amount of doping is approximately linear for the three low-energy bands, while the two high-energy peaks are nearly constant. This result is only qualitative because the band heights, in the same crystal, vary by about a factor of two in the different parts of the crystal with the top of the boule less doped than the bottom. An example of this difference is shown in Fig. 3 and can be explained by a segregation coefficient for  $\text{Ce}^{3+}$  of about 0.2, responsible for the increasing of the impurity concentration in the melt during the growth and henceforth in the lower part of the crystal boule. Even within these uncertainties, the different behavior upon Ce doping of the two high-energy bands compared to that of the lower-energy bands is the first indication of the presence of different centers responsible for the two sets of bands. All the absorption bands are present only in  $\text{Ce}^{3+}$  doped crystal and we think very unlikely that a different, unwanted impurity could be present in about the same concentration. The  $\text{CeF}_3$ -powder purity was indeed at least 99.9% and the presence of  $\text{Eu}^{2+}$  as a trace impurity, as revealed by the emission spectra, cannot account for the observed absorption structures. We suggest therefore that  $\text{Ce}^{3+}$  ions form different centers in  $\text{KMgF}_3$  crystals, as discussed

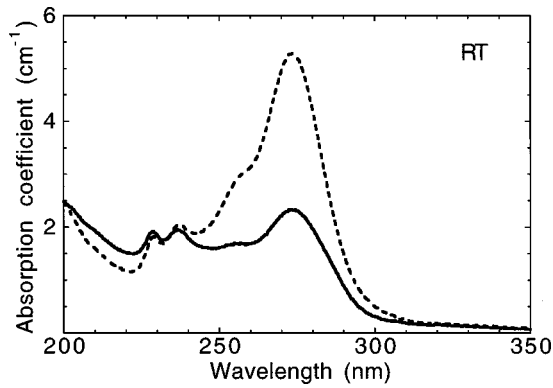


FIG. 3. Absorption spectra of  $\text{KMgF}_3:\text{Ce}^{3+}$  at room temperature for two different portions of the crystal boule. The top of the boule produces the spectrum shown by the solid line, whereas the dashed line refers to the bottom of the boule, with a higher concentration of dopant.

below. Thermal treatment (annealing at 1000 °C for two hours and quenching to room temperature) does not change the absorption spectrum, ruling out the hypothesis of the formation of  $\text{Ce}^{3+}$  dimers or larger aggregate centers.

### B. Emission

Also the emission spectra confirm the existence of two kinds of  $\text{Ce}^{3+}$  centers. At all temperatures, the excitation at 271, 255, and 245 nm originates a broad asymmetric emission peaked at 352 nm, as shown in Fig. 4. The spectrum can be decomposed into the sum of two Gaussian bands whose maxima are separated by approximately  $1770\text{ cm}^{-1}$ . The emission excited in the high-energy bands at 227 and 234 nm is shown in Fig. 5. Three emission bands are present at 264, 283, and 352 nm. The latter is the asymmetric band just described and its presence is due to the process of reabsorption by the 271-nm absorption band of the luminescence emitted in the 265–285 nm region. Thus the two absorption bands peaked at 227 nm and 234 nm have their own emission in the region 260–290 nm. The decay times were measured at three different temperatures, namely 80 K, 170 K, and 295 K, and at the three emission wavelengths of 280 nm, 340 nm, and 374 nm. The results are summarized in Table I

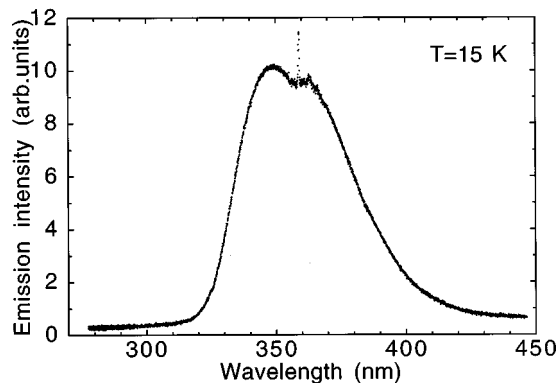


FIG. 4. Emission spectrum of  $\text{KMgF}_3:\text{Ce}^{3+}$  at low temperature, excited at 271 nm. The sharp peak at 359 nm together with the Stoke vibronic structures from 360 nm to 370 nm are due to trace impurities of  $\text{Eu}^{2+}$ .

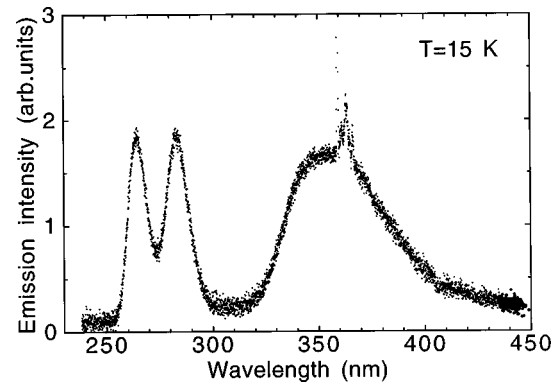


FIG. 5. Emission spectrum of  $\text{KMgF}_3:\text{Ce}^{3+}$  at low temperature, excited at 234 nm. See the caption of Fig. 4 for the 360–370 nm structures.

and they show that all decay times are essentially temperature independent. Moreover a marked difference in the values of the decay time is observed between the 260–290 nm emission and that peaking at 350 nm. Throughout this latter emission no measurable variation of the decay time could be detected. Figure 6 reports an example of the decays at room temperature for the two emissions, showing the single-exponential decay of both transitions.

### C. Excitation

The excitation spectra of both luminescences have been measured up to 180 nm (6.9 eV) at various temperatures. The excitation of the 350-nm emission band basically reproduces the absorption spectrum without revealing any new feature. A further broad emission centered around 410 nm was found in the VUV experiment, whose excitation is centered around 190 nm. The presence of this band can be guessed at from the data of Fig. 2 which show a marked increase of the absorption at short wavelengths. The presence of oxygen-related centers in the  $\text{KMgF}_3$  crystal has been shown to be responsible for absorption in this spectral region.<sup>19</sup> Because this emission is not present in any of the  $\text{Ce}^{3+}$  excitation bands we did not further investigate this feature. The excitation of the 264 and 285 nm emissions is shown in Fig. 7 and it reveals, in addition to the 227- and 234-nm peaks found in absorption, two weak structures at 210 and 203 nm not visible in the absorption spectrum.

Two-photon excitation spectra give in the  $\text{KMgF}_3:\text{Ce}^{3+}$  system a limited amount of new information. The main absorption bands related to  $4f \rightarrow 5d$  transition are one-photon parity allowed and in strict cubic crystal field they are two-photon parity forbidden. If the symmetry is lower than cubic,

TABLE I. Measured decay times of the luminescence of  $\text{Ce}^{3+}$  in  $\text{KMgF}_3$  for different excitation and emission wavelengths, at three temperatures.

$\lambda_{\text{exc.}}$ (nm)	$\lambda_{\text{emis.}}$ (nm)	decay times (ns)		
		$T=80\text{ K}$	$T=170\text{ K}$	$T=295\text{ K}$
228	280	19.8	18.6	21.6
275	340	50.0	52.6	51.0
275	374	50.5	50.0	49.5

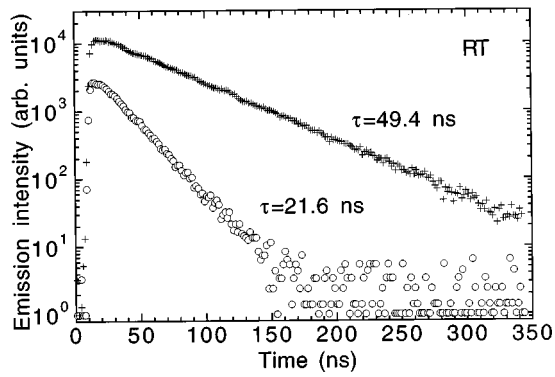


FIG. 6. Decay curves of the luminescences of  $\text{KMgF}_3:\text{Ce}^{3+}$  at room temperature. Open circles:  $\lambda_{\text{exc}} = 228$  nm,  $\lambda_{\text{emission}} = 280$  nm. Crosses:  $\lambda_{\text{exc}} = 275$  nm,  $\lambda_{\text{emission}} = 374$  nm. The excitation pulse was of about 10-ns duration.

due to the presence of charge compensating defects, these transitions can be observed with both kinds of excitations, but we do not expect the variety of the two-photon allowed (and one-photon forbidden)  $4f^n \rightarrow 4f^{n-1}5d$  transitions observed for example in other RE impurities. The two-photon excitation spectrum is shown in Fig. 8. As expected one can again reveal the  $\text{Ce}^{3+}$  bands at 271, 255, and 245 nm, but no excitation was found in the region 220–240 nm indicating that the two-photon absorption cross section for this latter centers is at least two order of magnitude smaller than that of the 271-nm band. The small signal due to the second-order process and the overall small concentration of impurity ions prevented us from analyzing the polarization dependence of the two-photon excitation spectra.

#### IV. DISCUSSION

As shown by the extensive literature quoted in the Introduction, the spectroscopic features of the  $\text{Ce}^{3+}$  ion depend strongly on the host crystal, on the crystal-field strength, and on the symmetry of the crystal site. All of these parameters, often not completely known, seldom allow a complete description of the system. The constant feature observed in almost all  $\text{Ce}^{3+}$  transitions in ionic crystal is the presence of four or five bands assigned to the crystal-field split  $5d$  level. In our case only three bands can be assigned to  $\text{Ce}^{3+}$  ions in the majority site. In  $\text{KMgF}_3$  the ionic radius of  $\text{Ce}^{3+}$  is 1.03

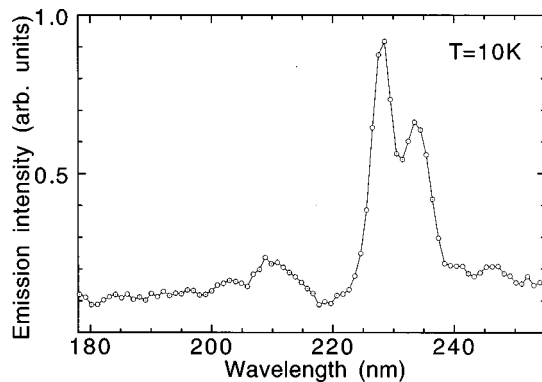


FIG. 7. Low temperature excitation spectrum of the  $\text{KMgF}_3:\text{Ce}^{3+}$  luminescence at  $\lambda_{\text{emission}} = 265$  nm.

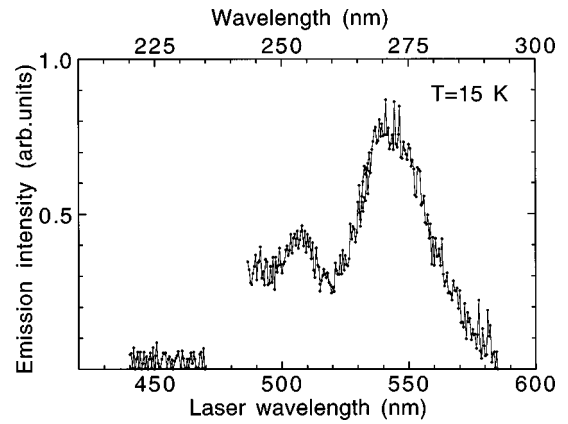


FIG. 8. Low temperature two-photon excitation spectrum of the  $\text{KMgF}_3:\text{Ce}^{3+}$  luminescence at  $\lambda_{\text{emission}} = 350$  nm. Data points in the region from 220 nm to 235 nm (laser wavelength from 440 nm to 470 nm) are indistinguishable from the noise of the apparatus.

$\text{\AA}$ , and it is smaller than the  $\text{K}^+$  radius (1.33  $\text{\AA}$ ) but much larger than that of  $\text{Mg}^{2+}$  (0.66  $\text{\AA}$ ). From the point of view of the ion site it is thus more likely that the  $\text{Ce}^{3+}$  substitutional site is the potassium site. In this case however two positive charges must be compensated. The most likely electrical compensators are the introduction of two  $\text{K}^+$ -ion vacancies, interstitial  $\text{F}^-$  ions, or two  $\text{O}^{2-}$  impurities at the  $\text{F}^-$  sites. In all cases the symmetry of the  $\text{Ce}^{3+}$  site is lowered from the cubo-octahedral one of the potassium site in the perfect perovskite lattice, to a tetragonal or orthorhombic symmetry. The presence in  $\text{KMgF}_3$  of  $\text{Ce}^{3+}$  centers with three different configurations, even if different from ours, was originally suggested by Ibragimov, Fazlizhanov, Falin, and Ulanov<sup>14</sup> to interpret the ESR data of this system. We assume that the presence of  $\text{K}^+$ -ion vacancies is the most likely way of charge compensation (like in alkali halides doped with divalent impurities) and that the majority site responsible for the 271, 255, and 245 nm bands is one with the two  $\text{K}^+$  vacancies along the  $C_{4v}$  axis. The two missing bands of the five-fold splitting of the  $5d$  level may be hidden because of weak intensity or buried under the next higher-energy bands. The assignment of the higher-energy bands in absence of more detailed information [as, for example, through an extended x-ray absorption fine structure (EXAFS) experiment] is only tentative. The kind of saturation in the number of centers for this minority site leads us to suppose an exhaustion of some ingredient of the center or of the available sites. In the first case one could think to the oxygen compensated centers and suppose a limited amount of oxygen in the melt under Ar atmosphere. The number of these  $\text{Ce}^{3+} + 2\text{O}^{2-}$  centers is therefore limited. Another possibility is the presence of the  $\text{Ce}^{3+}$  ion in the perfect cubo-octahedral site with the charge compensating vacancies far removed from the  $\text{Ce}^{3+}$  ion. It is clear that this configuration quickly saturates because the vacancies introduced begin to perturb one or the other of the perfect cubo-octahedral sites. We favor this interpretation since it involves only intrinsic constituent of the crystal and because, as one should expect, the high-symmetry site has transition energies higher than the vacancy-perturbed site.

Further support for the hypothesis of the two distinct types of  $\text{Ce}^{3+}$  centers is provided by our two-photon excitation spectra. The one-photon  $4f \rightarrow 5d$  transition is parity al-

lowed, and unlike the  $4f \rightarrow 4f$  two-photon transitions, it is parity forbidden in second-order perturbation theory. This selection rule is relaxed if the center lacks the inversion symmetry. This condition, in the case of Ce<sup>3+</sup> hosted in cubic crystals, is usually fulfilled with the aid of additional defects, namely charge compensating ones, bound to the trivalent impurity ion. In this way the site symmetry is lower than cubic, and the resulting odd-parity crystal-field perturbation mixes the  $4f$  ground state and the  $5d$  excited state wave functions, thus making possible the two-photon transitions among these states. This relaxation of the parity selection rule has been previously assumed in the discussion of Ce<sup>3+</sup>:CaF<sub>2</sub> two-photon  $4f \rightarrow 5d$  transitions,<sup>15,16</sup> and of Pr<sup>3+</sup>:Y<sub>3</sub>Al<sub>5</sub>O<sub>12</sub> (YAG) two-photon  $4f^2 \rightarrow 4f5d$  transitions.<sup>20</sup> In the former system, the marked polarization anisotropy of the zero-phonon nonlinear transition, confirmed the local C<sub>4v</sub> symmetry of the Ce<sup>3+</sup> ion, and, together with the measurement of the absolute cross section, opened the way to the refinement of the theoretical interpretation of the rare-earth two-photon  $4f \rightarrow 5d$  transitions.<sup>21-23</sup>

In our case, the lack of any detectable two-photon absorption in the region of the one-photon 227- and 234-nm peaks, is in agreement with the  $O_h$  site symmetry, proposed for this type of centers. The other Ce<sup>3+</sup> center, possessing the C<sub>4v</sub> symmetry, is of the same kind of that investigated by Gayen and Hamilton,<sup>15</sup> although some difference should be pointed out: in KMgF<sub>3</sub>, the single optically active electron of Ce<sup>3+</sup> shows a stronger coupling of the excited  $5d$  state with the surrounding lattice, resulting in broad absorption bands with a Gaussian line shape, and no zero-phonon lines and phonon sidebands as in CaF<sub>2</sub>. Another difference is that the charge compensating defects we propose are cationic vacancies, whereas in the CaF<sub>2</sub> host they are interstitial F<sup>-</sup> ions. This fact could be of interest in the theoretical discussion of dynamical ligand-polarization contributions to the two-photon cross section.<sup>22</sup> For the latter point, polarization anisotropy and absolute cross section need to be measured, but the small concentration we achieved of noncubic Ce<sup>3+</sup> centers, made those measurements unfeasible. The two models of luminescent Ce<sup>3+</sup> centers in KMgF<sub>3</sub>, are shown in Fig. 9, where the perturbed center is depicted according to our interpretation.

The crystal field in the KMgF<sub>3</sub> cubo-octahedral site is very small and this fact could explain the observed width of the  $5d$  manifold of about 6800 cm<sup>-1</sup>. The perturbed site shows a similar splitting of ~5000 cm<sup>-1</sup> although the real value is eventually larger than this, considering that not all of the  $5d$  components are resolved in our spectra. These values of the width of the Ce<sup>3+</sup>  $5d$  level are among the lowest found for this ion hosted in ionic crystals, where splittings of about 10 000 cm<sup>-1</sup> are normally found. The peculiar twelve-fold coordination at the KMgF<sub>3</sub> potassium site was shown to be responsible for the unusually small Stark splitting of the  $4f$   $J$  manifolds in the case of doubly ionized europium.<sup>24</sup> The two emission bands at 264 and 283 nm, identified as belonging to the cubic center, are separated by 2500 cm<sup>-1</sup> which is a rather large value for the spin-orbit splitting of the  $4f$  ground state.<sup>25</sup> A smaller value, closer to that found in other hosts, is obtained if the emission line shape is corrected for the reabsorption due to the perturbed site.

The order of magnitude of the emission lifetime is temperature independent as that of the same allowed transition in

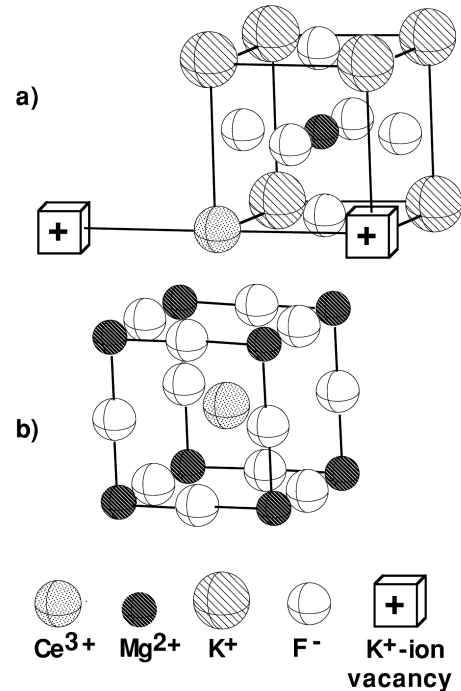


FIG. 9. Structure of the two luminescent Ce<sup>3+</sup> centers in the KMgF<sub>3</sub> crystal: (a) the origin of the crystal unit cell is at the impurity site, with the two K<sup>+</sup>-ion vacancies on the C<sub>4v</sub> axis; (b) the impurity ion is at the cubic site with the origin of the crystal unit cell at the Mg<sup>2+</sup> site. In both cases the Ce<sup>3+</sup> ion substitutes a K<sup>+</sup> ion.

other host crystals and is only slightly longer than those. Literature data report values from 23 ns in BaThF<sub>6</sub> (Ref. 26) to 40 ns in LiYF<sub>4</sub>,<sup>5</sup> and BaF<sub>2</sub>.<sup>27</sup> Furthermore the values of the decay times of the cubic and the perturbed Ce<sup>3+</sup> centers in KMgF<sub>3</sub> are consistent with the values found in the case of CeF<sub>3</sub> by Pedrini, Moine, Gacon, and Jacquier<sup>8</sup> who report decay times of 20 ns for regular and 35 ns for perturbed Ce<sup>3+</sup> centers. In spite of the higher concentration of perturbed centers compared to that of Ce<sup>3+</sup> cubic centers, the latter do not show a shortening of the decay time as the temperature is increased, as was the case in CeF<sub>3</sub>, where nonradiative energy transfer between different centers took place.<sup>28</sup> In our case, any diffusion of the excitation can be excluded due to the very low concentration of the different centers, and also a single-step transfer process cannot take place in the KMgF<sub>3</sub> lattice, where cubic and perturbed Ce<sup>3+</sup> centers do not reside one close to the other.

## V. SUMMARY

The spectroscopic properties of Ce<sup>3+</sup> ions entering substitutionally in the KMgF<sub>3</sub> fluoroperovskite lattice, have been investigated in detail. It has been shown that at least two sites are possible for the Ce<sup>3+</sup> ion with different absorption and emission properties. One site is the K<sup>+</sup> substitutional site with the perfect cubo-octahedral  $O_h$  symmetry and the other one is the same site with two perturbing K<sup>+</sup>-ion vacancies, which lower the local symmetry to the C<sub>4v</sub> orthorhombic. The charge difference between the impurity ion and the host-crystal substitutional site is probably the main reason for the low level of doping obtained.

- <sup>1</sup>E. Loh, *Phys. Rev.* **154**, 270 (1967).
- <sup>2</sup>N. Sarakura *et al.*, *Opt. Lett.* **20**, 294 (1995).
- <sup>3</sup>D. J. Ehrlich, P. F. Mouldon, and K. M. Osgood, Jr., *Opt. Lett.* **4**, 184 (1979).
- <sup>4</sup>D. J. Ehrlich, P. F. Mouldon, and K. M. Osgood, Jr., *Opt. Lett.* **5**, 339 (1980).
- <sup>5</sup>F. Okada, S. Togawa, K. Ohta, and S. Koda, *J. Appl. Phys.* **75**, 49 (1994).
- <sup>6</sup>K. H. Yang and J. A. De Luca, *Appl. Phys. Lett.* **31**, 594 (1977).
- <sup>7</sup>W. W. Moses, S. E. Derenzo, *IEEE Trans. Nucl. Sci.* **NS36**, 173 (1989).
- <sup>8</sup>C. Pedrini, B. Moine, J. C. Gacon, and B. Jacquier, *J. Phys.: Condens. Matter* **4**, 5461 (1992).
- <sup>9</sup>W. J. Manthey, *Phys. Rev. B* **8**, 4086 (1973).
- <sup>10</sup>L. R. Elias, W. S. Heaps, and W. M. Yen, *Phys. Rev. B* **8**, 4989 (1973).
- <sup>11</sup>M. A. Dubinski *et al.*, *Laser Phys.* **3**, 216 (1993).
- <sup>12</sup>M. A. Dubinski *et al.*, *J. Mod. Opt.* **40**, 1 (1993).
- <sup>13</sup>C. D. Marshall *et al.*, *J. Opt. Soc. Am. B* **11**, 2054 (1994).
- <sup>14</sup>I. R. Ibragimov, I. I. Fazlizhanov, M. L. Falin, and V. A. Ulanov, *Fiz. Tverd. Tela (Leningrad)* **34**, 3261 (1992) [*Sov. Phys. Solid State* **34**, 1745 (1992)].
- <sup>15</sup>S. K. Gayen and D. S. Hamilton, *Phys. Rev. B* **28**, 3706 (1983).
- <sup>16</sup>S. K. Gayen, G. J. Pogatshnik, and D. S. Hamilton, *J. Lumin.* **31/32**, 260 (1984).
- <sup>17</sup>J. C. Gacon, J. Baudry, C. Garapon, and G. W. Burdick, *Radiat. Eff. Defects Solids* **135**, 41 (1995).
- <sup>18</sup>G. H. Dieke, *Spectra and Energy Levels of Rare Earth Ions in Crystals* (Wiley, New York, 1968).
- <sup>19</sup>F. Fioravanti *et al.*, *Proceedings of the XII International Conference on Defects in Insulating Materials*, edited by O. Kanert and J. M. Spaeth (World Scientific, Singapore, 1993), p. 574.
- <sup>20</sup>S. K. Gayen, Bin Qing Xie, and Y. M. Cheung, *Phys. Rev. B* **45**, 20 (1992).
- <sup>21</sup>S. K. Gayen, D. S. Hamilton, and R. H. Bartram, *Phys. Rev. B* **34**, 7517 (1986).
- <sup>22</sup>R. C. Leavitt, *Phys. Rev. B* **35**, 9271 (1987).
- <sup>23</sup>A. G. Makhanev, V. S. Korolkov, and L. A. Yuguryan, *Phys. Status Solidi B* **149**, 231 (1988).
- <sup>24</sup>R. Francini *et al.*, *Phys. Rev. B* **55**, 7579 (1997).
- <sup>25</sup>B. G. Wybourne, *Spectroscopic Properties of Rare Earths* (Wiley, New York, 1965).
- <sup>26</sup>P. Mesnard *et al.*, *Chem. Phys. Lett.* **229**, 139 (1994).
- <sup>27</sup>Xu Zizong *et al.*, *Nucl. Instrum. Methods Phys. Res. A* **322**, 239 (1992).
- <sup>28</sup>M. Nikl and C. Pedrini, *Solid State Commun.* **90**, 155 (1994).